Arch. Metall. Mater., Vol. 61 (2016), No 3, p. 1291–1296

DOI: 10.1515/amm-2016-0213

M. KRÓL*#, T. TAŃSKI*

SURFACE QUALITY RESEARCH FOR SELECTIVE LASER MELTING OF TI-6AL-4V ALLOY

One of the innovative technology of producing the components is Selective Laser Melting (SLM) belongs to additive manufacturing techniques. SLM technology has already been successfully applied in the automotive, aerospace and medical industries. Despite progress in material flexibility and mechanical performances, relatively poor surface finish still presents a significant weakness in the SLM process.

The scope of the present article is the study the influence of selective laser melting parameters such as laser power, scanning speed, exposure time and hatch spacing through additive manufacturing as well as the orientation of the model corresponding to the laser beam on the surface characteristic of the components made from Ti-6Al-4V alloy. By using optimized process parameters, a low surface roughness can be obtained.

In research, the machine for the selective laser melting of metal powders Renishaw AM 125 device was used. Based on experiment plan, 32 models were produced, which were examined to define the surface roughness and thus represent an influence of process parameters and the orientation on the model surface quality.

The article discusses the fundamental factors determining the roughness that gives invaluable knowledge to improve the surface quality of SLM parts.

Keywords: additive manufacturing; SLM process; surface quality; roughness.

1. Introduction

Additive Manufacturing (AM) is a recent innovation in manufacturing technology with development beginning in the mid-1980's [1]. Selective Laser Melting (SLM) is an additive manufacturing method that uses a laser in an inert atmosphere to selectively melt layers of loose metal powder into a solid, building a part layer by layer from the bottom up [2, 3]. Selective laser melting and electron beam melting typically utilize the entire melting mechanism that completely dissolved all particles of metal powder and generates a compact and stable solid body [4, 5]. The powder material is subjected to a series of complicated chemical and physical phenomena such as oxidation, wetting, epitaxial solidification, and vaporization. Thermal energy from succeeding scans of a laser or electron beam is typically adequate to re-melt a portion of the earlier solidified solid structure. That type of complete melting is highly useful for producing well-bonded, high-density structures from engineering metals [6, 7]. In selective laser melting, a singular component powder is melted and crystallized by scanning of a CO_2 or an Nd-YAG laser onto powder bed, which is different from selective laser sintering (SLS) that uses metal particles encapsulated with a polymer or a combination of various metal powders of low and high melting points [8, 9]. SLM is a layer-wise material addition method that enables complex 3D solid model production by selectively consolidating successive layers of pre-deposited powder, each corresponding to particular slice from the CAD design. The consolidation is accomplished by thermal energy supplied by a focused and PC controlled laser emission. For the production of practical metallic models, machines or devices, high density is desired, and this can be achieved from SLM without any post-processing steps. The additive manufacturing of metal elements by rapid prototyping looks to be suitable for small or single lot production and small-sized parts of complex geometry [5, 8].

Selective laser melting as a layer additive production processes is utilized in various industry sectors, such as a motor racing, automotive, aerospace, medical appliances, etc. Titanium and its alloys are regarded to be excellent materials for the implant since of their associated biocompatibility and high strength to weight ratio. This broad utilization range principally affected by the advantage of SLM technology: short design and production cycle; complex shape and hollow parts; a variety of implementation materials, etc. Due to its usefulness of materials and forms, the primary benefit of SLM is to create metal complex-shaped elements in one step, however it also has drawback that require precise process control: the high-temperature gradients and densification ratio through the process yield high internal stresses or part distortion: the risk of balling formation in the melt pool can result in inadequate surface roughness [10-14].

Reduction of surface roughness is one of the fundamental research issues within the additive manufacturing technique SLM since one of the main cost factors is the post processing of surfaces. The surface roughness depends on several factors: material, powder particle size, layer thickness, laser and scan

* SILESIAN UNIVERSITY OF TECHNOLOGY, INSTITUTE OF ENGINEERING MATERIALS AND BIOMATERIALS, FACULTY OF MECHANICAL ENGINEERING, 18 A KONARSKIEGO STR., GLIWICE 44-100, POLAND

Corresponding author: mariusz.krol@polsl.pl

parameters, scan strategy, the orientation of the component in the building chamber and surface post-processing [15, 16]. Laser power defines the severity of the temperature gradient, and due to this temperature rise, melting of the powder takes place. Therefore, the level of power has a meaningful effect on the surface quality. Scan speed also determines the amount of energy input during the melting and consequently contributes towards the surface quality of the part. Orientation and layer thickness causes "stair effect" in SLM parts that lead to the poor surface finish. Hatch distance has also been found to affect the surface roughness of the SLM models. Because of the "balling effect" and "stair effect" due to the layer-additive production, surface roughness of sloping plane depends on the processing parameters and the tilted angle. Also, the roughness of top surface differs strongly from the roughness of side surfaces [15, 17, 18]. To overcome this problem, a variety of surface modification techniques are available in the market including mechanical processes, chemical processes, and thermal processes [1, 16, 19, 20].

In this study, experimentally selected SLM process conditions and orientation of models made by Ti-6Al-4V alloy to ensure a minimum average and total roughness values. In fact, in literature, there is still little-detailed information regarding the titanium parts produced by SLM process.

2. Experimental procedure

the material for the experiment was Ti-6Al-4V alloy supplied by Renishaw. Currently, no literature reports on the optimized processing parameters for this specific powder. The material had the chemical composition listed in Table 1.

TABLE 1
Chemical composition of Ti-6Al-4V powder used in the experiments, wt. %

	Al	V	C	Fe	Ti	N	O
Ti-6Al-4V	5.5-6.75	<0.4	<0.1	<0.3	Balance	Trace	Trace

Renishaw Ti-6Al-4V (Grade 23) fine powder had the flowability 43.9 s according to the PN-82/H-04935 standard, the apparent density 2.61 g/cm3 according to the PN-EN ISO 3923-1:2010 standard and tapped density 2.79 g/cm^3 according to the PN-EN ISO 3953:2011E standard. Figure 1 shows the morphologies of the Ti-6Al-4V powders. As shown, the as-received titanium fine powder is dominantly regular with spherical shaped particles. Morphology analysis was conducted, and the results in the vicinity of the 10th, 50th, and 90th percentile for size were reported and values were found to be approximately 17.99 µm, 32.01 µm, and 53.02 µm, respectively.

The samples were carried out on a Renishaw AM125 machine that employs a pulsed Nd: YAG laser with wavelength 1070 nm with the maximum average power of 200 W and a spot size of 35 µm. The device is also equipped with two oxygen sensors to ensure low oxygen content during the manufacturing process. Before starting the process itself, the chamber is flooded with 99.996 % pure Argon until a value below 0.1% oxygen is reached. During the manufacturing of the specimens, the chamber was continually flooded with Argon guaranteeing a low oxygen content. With that process, an oxygen content of around 100 ppm could be achieved. A pure titanium base plate was used for creating samples and was polished before the process to guarantee a good adhesion of the powder and was heated up to 150°C and was kept at this level during manufacturing process until models were complete.

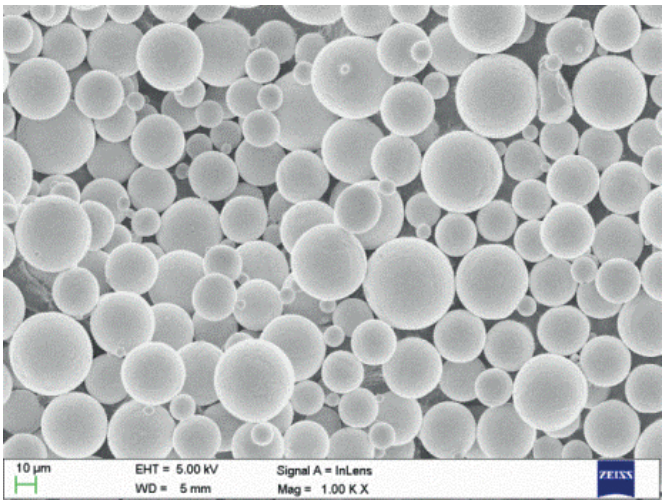

Fig. 1. SEM image showing characteristic morphologies of Ti-6Al-4V fine powder

Cubic specimens with an edge length of 10 mm were generated for the evaluation of surface quality (Fig. 2). Four main process parameters at four levels were chosen for study: laser power, scan speed, exposure time and hatch spacing. These factors define the energy delivered by the laser beam to a volumetric unit of powder material. To produce a good functional part, it is necessary that the particles on the part bed surface receive a satisfactory amount of energy through the laser melting process. These parameters have a complicated confusing effect during the laser melting process when all of the parameters are modified in an experiment. The melt pool variety and defect generation will be easily characterized if some parameters are kept constant.

To find out the influence of SLM parameters on roughness, two series of samples were made. As a first set, 16 parts were built with parameters presented in Table 2 to find out which set of laser power and scanning speed lowers the surface roughness most. After establishing laser power and scanning speed, next series of samples was prepared. The layer thickness approx. 30 µm was constant for both series of samples. Representative platform with created models is presented in Fig. 2.

TABLE 2
Two series of samples made under SLM process conditions

Parameter	First set, value	Second set, value
Laser Power (W)	75, 100, 125, 150	150
Scanning speed (mm/s)	200, 230, 260, 290	290
Hatch spacing (µm)	25	25, 50, 75, 100
Exposure time (µs)	100	25, 50, 75, 100

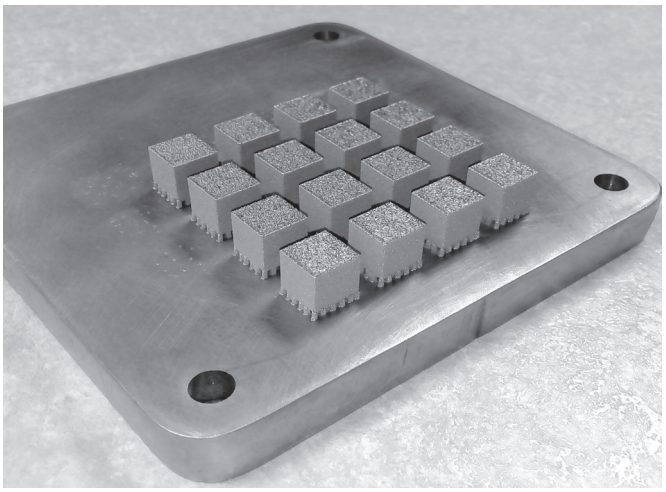

Fig. 2. Representative platform with created models

Before the roughness measurement, samples were placed in an ultrasonic bath for 15 minutes. The measurements of the roughness of top and side surfaces were carried out on the profilographometer Sutronic 25 of Tylor-Hubson Company. Bottom surfaces are not analyzed because the surface that is investigated has to be supported. It was assumed the measurements length was 4 mm and measurement accuracy was ±0.01 μm. The parameter Ra acc. the Standard PN-EN ISO 4287:1999 was assumed as the quantity characterizing the roughness. It was carried out five measurements on each of the investigated samples on a top surface and a side surface and inclination at different areas to avoid adulteration of the metered values, and it was determined the average, standard deviation and confidence interval, assuming the confidence factor at 1-α=0.95.

After determining the effect of processing parameters on roughness, optimal manufacturing parameters were selected. Geometry was designed to measure roughness surfaces inclined to the horizontal at "sloping angles" in the range 0÷90° at 10° intervals (Fig. 3). This similar geometry was used in previous works [16, 19], because it allows the surface roughness for each inclination angle to be easily measured.

a)

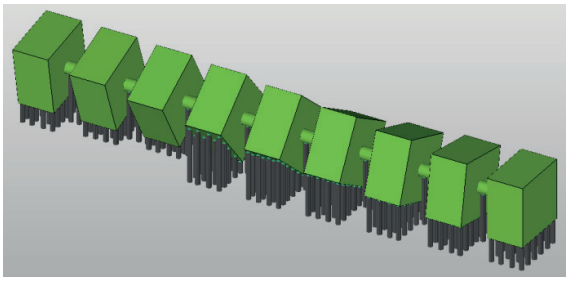

b)

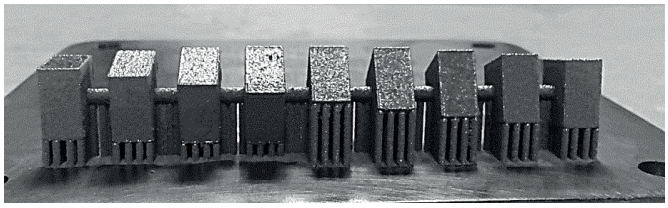

Fig. 3. Test part fabrication: (a) test part CAD model; (b) fabricated test part

3. Results and discussion

Figure 4 illustrates the characteristic surface morphologies of SLM processed titanium alloy representative parts observed at a relatively low magnification produced under the first set of parameters given in Table 2. Continuous scan tracks with a certain amount of spherical particles were formed. Small sized metallic particles with a diameter of 7.5 of micrometers were occasionally observed on the surfaces (balling effect). The balling effect is a complex metallurgical process comes from non-optimal SLM manufacturing parameters and material properties of the powder. This adverse effect may result in breaking up the liquid scan track during SLM and produce particles in spherical shapes. This phenomenon and unbalanced viscosity may cause homogeneous deposition of the subsequent fresh powder layer and even causes delamination due to weak bonds between grains and layers. This effect is also caused by floating powder particles in the chamber due to the flow of argon during the manufacturing process. Small welded particles can be melted together with recoated powder particles. However, large particles, which attach to the top surface, can be easily touched and removed by a recoating wiper. Due to its unusual formation, this defect is distributed stochastically in the specimen, instead of directly being correlated with processing parameters. Based on the observation of LM images it was found that with increasing the laser power, the amount of welded particles gradually reduced. No voids were found in analyzed surfaces. Interestingly, at a reasonable P of 150 W, a clear and regular liquid solidification front free of balling phenomenon was observed, yielding stable and continuous scan track (Fig. 4d).

The roughness measurements of top and side surface under various processing conditions (Table 2) are presented in Figure 5. It can be seen that laser power has a significant effect on the roughness of metal samples. When laser power is 150 W, all of the roughness values reflecting roughness quality are minimal on the condition of scan speed at 290 mm/s. When laser power is lower than 150 W, top and side surface roughness values increases sharply, which means that top and side surface quality degrades, and the stability of process reduces. As can be seen in Fig. 5a decreasing scan speed resulted in an increase of roughness when a constant value of laser power was used. However, a different trend of roughness was shown for the laser power of 125 W and 150 W. At first, the roughness of samples increased as scan speed decreased. When it reaches a scan speed of 260 mm/s, the roughness started to fall and again rise with the reduction in scan speed. Fig. 5 also shows that the rate of change of roughness with the scan speed is greater as laser power increases, over the range tested here. Moreover, the surface quality of side walls is less than the quality of top surfaces because of several sintered powder particles.

The lowest roughness values of top and side surfaces were achieved for the sample prepared at 150 W and 290 mm/s and were 8.8±0.2 μm and 11.4±0.4 μm, respectively. These parameters were used for next experimental process and set as constant.

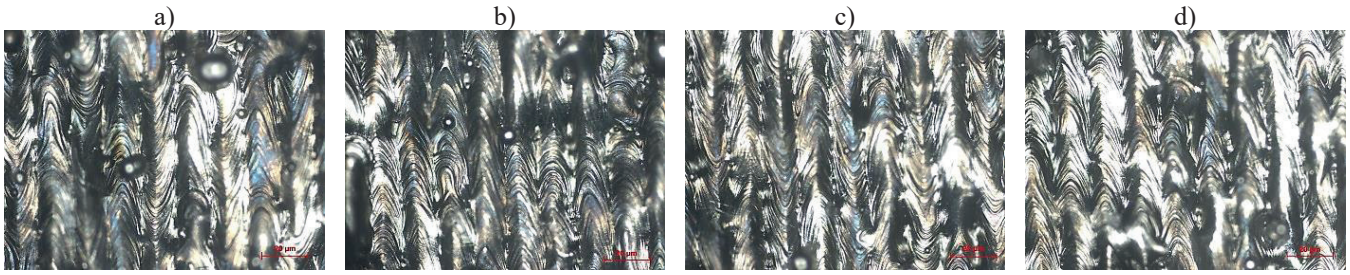

Fig. 4. Light microscope images represent the differences of SLM parts made with different values of laser power and scanning speed, mag. 1000x

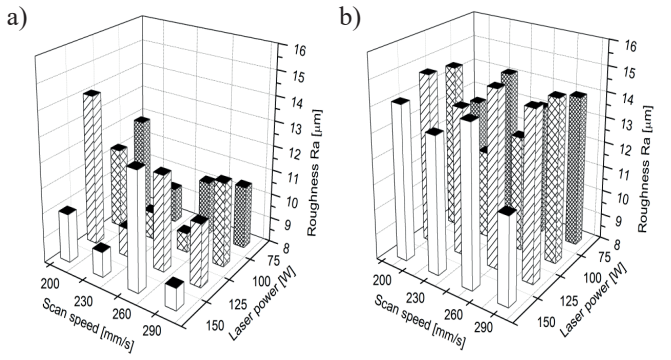

Fig. 5. Column diagram of Ra results for h=25 µm and t=100 µs: a) top surface; b) side surface

A solidified surface is shown in Fig. 6, which was fabricated under the second set of parameters given in Table 2. Some powder particles were melted to the top surfaces that are evident through the voids. The voids are randomly placed with irregular morphology along and between the hatch lines. Because the hatch spacing is increasing, the increased pool size results in increased overlap, which deteriorates the tops surface's roughness. On the other side, due to the reduced melt pool when melting the titanium alloy powder, laser irradiation causes not only larger melt pool but also extra heat that evaporates the molten materials. At a relatively high exposure time of 100 µs, an enormous amount of considerably small-sized balls with diameters below 10 µm was formed along the liquid solidification front implying the occurrence of balling effect at a microscopic scale. On increasing hatch spacing to 100 µs, the liquid solidification front started to become irregular, and a large number of balls were present (Fig. 6c and 6d). At large hatch spacing, the liquid solidification front became considerably disorderly, producing interrupted scan tracks.

In the case of the second series of samples, scan speed, and laser power is fixed at 290 mm/s and 150 W, respectively. A large number of experiments with hatch spacing 25, 50, 75 and 100 µm on the conditions of exposure time of 25, 50, 75 and 100 µs are operated for investigating the effects of processing condition on surface quality (Figure 7). When the exposure time is relatively low at 25 µs, hatch spacing naturally influences on quality of top and side surfaces. The roughness of top and side surfaces with an exposure time of 25 µs is minimal and increases sharply when exposure time increases to 100 µs. When hatch spacing is fixed at 25, 50, 75 and 100 µm W, generally side surface roughness increases with the increase of exposure time, which indicates that surface quality gets worse and worse with the rise of exposure time. Moreover, if was found that the surface quality of side walls are less than the quality of top surfaces.

The lowest roughness results of top and side surfaces were obtained with low-hatch spacing and low-exposure time values, yielding an improvement of top and side surface quality. The average Ra value of top surface for these parts was measured to be about 8.5 µm with a standard deviation of 1.5 µm, and 8.9 µm with a standard deviation of 1 µm for side surface. However, the lowest roughness result Ra=8.2±0.5 µm was found for side surface prepared with h=100 µm and t=50 µs, but top surface roughness was unsatisfactory and reached 10.9±0.6 µm. It may be caused by poor adhesion of the adherens particles to the side surface which dropped off as a result of ultrasonic cleaning and thereby decreased surface roughness of the side surface.

It is worth to notice that, in both series of processing conditions, the side surface roughness in the vertical path

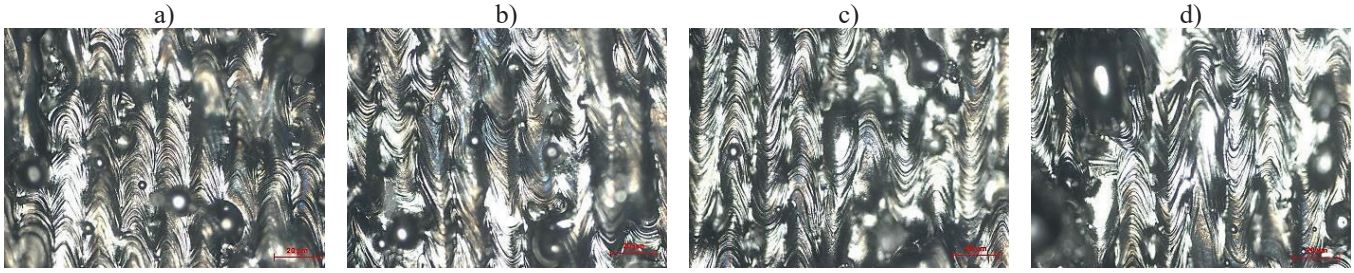

Fig. 6. Light microscope images represents the differences of SLM parts made: (a) h=25 µm, t=25 µs; (b) h=25 µm, t=100 µs; (c) h=100 µm, t=25 µs; (d) h=100 µm, t=100 µs; mag. 1000x

reached a higher value than that of the side roughness in the horizontal path. It could be a consequence of interlayer contacts between melted layers of powder rising Ra in this direction. Measuring side Ra along the horizontal axis will only take into consideration one layer. Measuring in the vertical axis measures across multiple layers, a melted interlayer connection has the potential to increase the roughness of side surfaces. The roughness of side surface of a model can also rise due to partly melted, entrained powder particles that adhere and agglomerate to the external edge of the solidified melt pool identified as "satellite formation" or "hillocks". Satellite formation mainly occurs when powder particles are not given enough time, heat or energy to penetrate the melt pool before melt pool solidification.

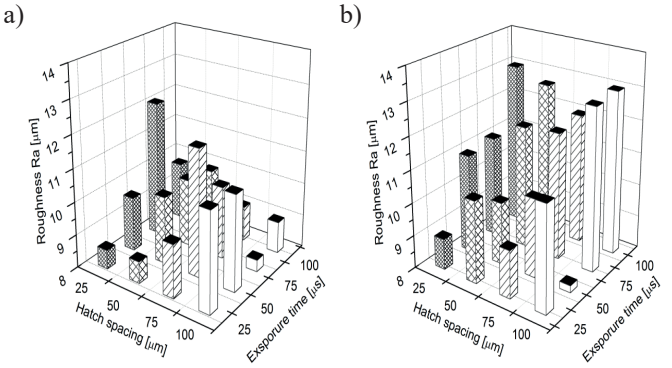

Fig. 7. Column diagram of Ra results for v=290 mm/s and P=150 W: a) top surface; b) side surface

As shown in Figures 6 and 7, the best surface quality in the average roughness were achieved by the following combinations of laser power 150 W, scan speed 290 mm/s, hatch spacing 25 µm and exposure time 25 µs.

To evaluate the surface quality of laser generated parts different orientations of the observed faces must be considered. While horizontal surfaces are formed by the upside of scanning tracks, the vertical faces are built into the side walls of the boundaries. Fig. 8 shows the two kinds of the classic surface morphology of SLM parts made with optimized parameters such as v=290 mm/s, P=150 W, h=25 µm, t=25 µs: (a) top surface and the (b) side surface. Based on the images, it can be observed that there are the significant differences in surface morphology between two types of walls. No voids were found in analyzed tops surface. A clear and regular liquid solidification front free of the balling phenomenon was observed, yielding stable and continuous scan track. Analysis of surface quality of side wall, semi-molten particles adhere to the side surface were found.

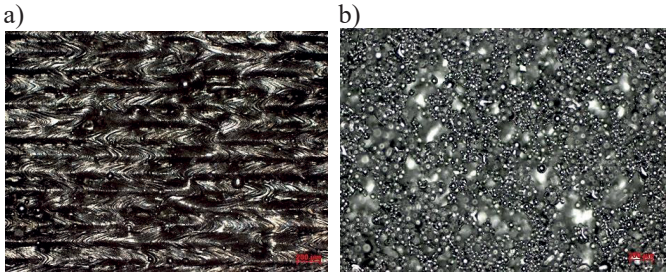

Fig. 8. Light microscope images represent the differences of SLM parts (inclination 0°) with (a) top surface and (b) side surface

Fig. 9. shows the variation in average surface roughness with the sloping angle, with error bars indicating the standard deviation at each angle across the datasets. This graph is obtained by measurements on the model (Fig. 3) made by SLM of titanium alloy. The measurements of roughness presented that the top surface (0° inclination) had the lowest roughness (Ra=7.5±0.5 µm), as expected. The surface roughness of 0° horizontal surface is generated by the rippling effect that occurs during the laser melting process. The surface roughness of side wall is obviously higher than that top surface. Thus, it can be considered that the adherent semi-molten particles on the side surface strongly increase the surface roughness and decrease the dimensional accuracy. It is important to notice that the side surfaces, unlike on top ones, laser remelting is not possible with SLM process, since the material can only be sintered horizontally. As the inclination angle increases from 0°, higher surface roughness results from the stair effect. The stair effect can be decreased by reducing the layer thickness or by the rising sloping angle. In both cases numerous stairs appear, however, the size of the stairs becomes smaller, causing lower surface roughness. The trend of measured roughness of the top surface is mainly constant in the range 10-60°. The tendency of a measured roughness of the designed and produced model can be defined as the result of rising presence of particles with surface inclination. At very low sloping angles, the appearance of particles with step edges does not considerable influence the morphology because the distance between consecutive step edges is much larger than the particle size. It indicates that some particles adhered on the step edges do not make a significant contribution to the surface roughness. As the sloping angles increases, edges become closer to each other generating the particle concentration to increase. The appearance of particles that partly fill the space between edges cannot be ignored, and in fact, it affects the measured roughness, generating it to be larger than expected from only the stair effect.

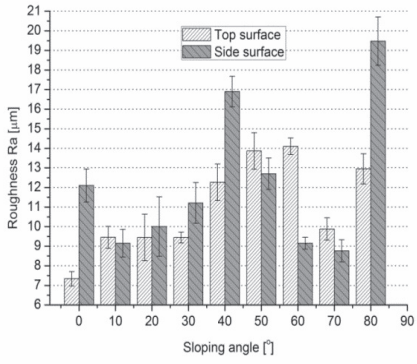

Fig. 9. Experimental roughness at different sloping angle

4. Conclusions

The effects of laser power, scan speed, hatch spacing and exposure time on the top and side surface roughness of Ti-6Al-4V parts produced by SLM were studied. To characterize the actual surface at different sloping angles, an individual geometry sample has been produced and analysis has been

conducted at surface profilometer. It was found that roughness is minimized when:

- the laser power is 150 W,
- the scan speed is 290 mm/s,
- the exposure time is 25 μs,
- the hatch spacing is 25 μm.

The process parameters are optimized to reduce roughness, leading to part roughness lower than 9 μm. The influence of sloping angle on surface roughness is studied, as well as the difference between top and side surface roughness. Dimensional analysis is conducted on designed model showing process accuracy below 9 μm. Based on achieved results, to obtain relatively low surface roughness of top and side walls of models produced by titanium, it is recommended to tilted models approx. 10-20 degrees relative to the substrate.

Acknowledgement

This publication was financed by the Ministry of Science and Higher Education of Poland as the statutory financial grant of the Faculty of Mechanical Engineering SUT.

REFERENCES

[1] B. Zhang, L. Zhu, H. Liao, Ch. Coddet, Appl Surf Sci. **263**, 777-782 (2012).
[2] S. Negi, S. Dhiman, R.K. Sharma, Rapid Prototyping J. **20**, (3), 256-267 (2014).
[3] I. Yadroitsev, L. Thivillon, Ph. Bertrand, I. Smurov, Appl Surf Sci. **254**, (4), 980-983 (2007).
[4] A.B. Spierings, N. Herres, G. Levy, Rapid Prototyping J. **17**, (3), 195-202 (2011).
[5] M. Król, M. Kujawa, L.A. Dobrzański, T. Tańsk, Archives of Materials Science and Engineering **67**, (2), 84-92 (2014).
[6] H. Attar, M. Calin, L.C. Zhang, S. Scudino, J. Eckert, Mat Sci Eng A-Struct. **593**, 170-177 (2014).
[7] S. Negi, R.K. Sharma, S. Dhiman, Mater Manuf Process. **30**, (5), 644-653 (2015).
[8] M. Król, P. Snopiński, B. Tomiczek, T. Tański, W. Pakieła, W. Sitek, P Est Acad Sci. **65**, (2), 107-116 (2016).
[9] D. Gua, Y.Ch. Hagedorn, W. Meiners, G. Meng, R.J.S. Batista, K. Wissenbach, R. Poprawe, Acta Mater. **60**, 3849-3860 (2012).
[10] A. Zieliński, M. Miczka, M. Sroka, Mater. Sci. Tech-Lond. (2016), DOI:10.1080/02670836.2016.1150242 (in press).
[11] H.K. Rafi, N.V. Karthik, H. Gong, T.L. Starr, B.E. Stucker, J Mater Eng Perform. **22**, (12), 3872-3883 (2013).
[12] G. Pyka, G. Kerckhofs, I. Papantoniou, M. Speirs, J. Schrooten, M. Wevers, Materials, **6**, 4737-4757 (2013).
[13] L. Wang, P. Liu, L. Wang, W. Xinga, Y. Fana, N. Xua, Mater Manuf Process. **28**, (11), 1166-1170 (2013).
[14] V. Seyda, N. Kaufmann, C. Emmelmann, Physics Procedia **39**, 425-431 (2012).
[15] L.A. Dobrzański, W. Sitek, M. Krupiński, J. Dobrzański, J Mater Process Tech. **157-158**, 102-106 (2004).
[16] E. Yasa, J. Deckers, J.P. Kruth, Rapid Prototyping J. **17**, (5), 312-327 (2011).
[17] K.A. Mumtaz, N. Hopkinson, Journal of Material Processing Technology **210**, 279-287 (2010).
[18] A. Daekeon, K. Hochan, L. Seokhee, J Mater Process Tech. **209**, 664-671 (2009).
[19] A. Zieliński, G. Golański, M. Sroka, Kovove Mater. **54**, (1), 61-70 (2016).
[20] P. Snopiński, T. Tański, K. Labisz, S. Rusz, P. Jonsta, M. Król, Int. J. Mater. Res. (2016), DOI:10.3139/146.111383 (in press).